to form spinel on each side of the reaction interface.

The three phases involved in the spinel-forming reaction, *i.e.* MgO, β-Ga_2O_3 and $MgGa_2O_4$, are essentially cubic close-packed oxygen structures. This precludes the need for the formation of an intermediate metastable phase whose oxygen arrangement or packing would enable a gradual transition from one type of oxygen packing to another, *e.g.* cubic close-packed to hexagonal close-packed.

It is of interest to note that although there is considerable analogy between topotaxy in metal and oxide systems, no comparable studies have been reported for metal systems for reactions of the type: $A+B\rightarrow C$.

The authors wish to thank Professor G. W. Brindley for his valuable discussions during the course of this investigation and for his critical review of the manuscript. This study was supported by the U.S. Air Force Office of Scientific Research, Solid State Science Division under Grant No. AF-AFOSR-208-63.

References

BARRETT, C. S. (1952). *Structure of Metals*. New York: McGraw-Hill.

BERNAL, J. D., DASGUPTA, D. R. & MACKAY, A. L. (1959). *Clay Mineral Bull.* **4**, 15–30.

BRINDLEY, G. W. (1963). *Prog. Ceram. Sci.* **3**, 1–55.

BÜSSEM, W. & KÖBERICH, F. (1932). *Z. phys. Chem.* B**17**, 310–326.

CARTER, R. E., ROTH, W. L. & JULIEN, C. A. (1959). *J. Amer. Ceram. Soc.* **42**, 533–536.

COTTRELL, A. H. (1955). *Theoretical Structural Metallurgy*, 2nd ed. London: Edward Arnold.

GELLER, S. (1960). *J. Chem. Phys.* **33**, 676–684.

KATZ, G. (1965). *Topotactic Reactions in Precipitation from, and Formation of Gallium Spinels*. Thesis, The Pennsylvania State Univ.

KATZ, G., NICOL, A. W. & ROY, R. (1969*a*). *Nature, Lond.* **223**, 609–610.

KATZ, G., NICOL, A. W. & ROY, R. (1969*b*). *Z. Kristallogr.* **130**, 388–404.

KATZ, G. & ROY, R. (1966). *J. Amer. Ceram. Soc.* **49**, 168–169.

KATZ, G. & ROY, R. (1970). *J. Cryst. Growth*, **6**, 221–227.

KOHN, J. A., KATZ, G. & BRODER, J. (1957). *Amer. Min.* **42**, 398–407.

SAALFELD, H. (1962). *Ber. Dtsch. Keram. Ges.* **39**, 52–54.

SAALFELD, H. & JAGODZINSKI, H. (1957). *Z. Kristallogr.* **109**, 87–109.

SWANSON, H. E., COOK, M. I., EVANS, E. H. & DE GROOT, H. H. (1960). *Standard X-Ray Diffraction Powder Patterns*, Circular 539, **10**, National Bureau of Standards, Washington, D.C.

SWANSON, H. E. & TATGE, E. (1953). *Standard X-Ray Diffraction Powder Patterns*, Circular 539, **1**, National Bureau of Standards, Washington, D.C.

WAGNER, C. (1936). *Z. phys. Chem.* B**34**, 300–316.

Acta Cryst. (1975). A**31**, 660

Transition of V_6O_{13} to VO_2 Observed with a High-Resolution Electron Microscope

BY SHIGEO HORIUCHI, MASANOBU SAEKI AND YOSHIO MATSUI

National Institute for Researches in Inorganic Materials, Sakura-mura, Niihari-gun, Ibaraki, 300-31 *Japan*

AND FUMIO NAGATA

Hitachi Central Research Laboratory, Kokubunji, Tokyo, 185 *Japan*

(*Received* 12 *August* 1974; *accepted* 20 *March* 1975)

Under irradiation by an intense electron beam a V_6O_{13} crystal reacts with the carbon deposited on the surface during microscopic observation. The structural changes during the reaction were directly observed by means of lattice images, in which the array of VO_6 octahedra was resolved. At the initial stage cavities smaller than 20 Å in diameter appear preferentially in the thin part of the crystal and some crystallographic shear planes are formed in their wall. The cavities with the heavily distorted surroundings are seen as white regions. Kinks in lattice fringes, indicating the occurrence of stacking faults, are simultaneously found in the matrix. At the advanced stage the VO_2 phase and its twin component are produced. The mechanism of the transition of V_6O_{13} to VO_2 can be interpreted in terms of the cooperative movement of octahedra.

Introduction

It is known for a vanadium–oxygen system that there are two series of Magnéli phase, *i.e.* V_nO_{2n-1} ($n=3$ to 8) between V_2O_3 and VO_2, and V_nO_{2n+1} ($n=3$ and 6) between VO_2 and V_2O_5 (Andersson, 1954; Stringer, 1965). Tilley & Hyde (1970) reported that a V_2O_5 crystal heated by the irradiation of an intense electron

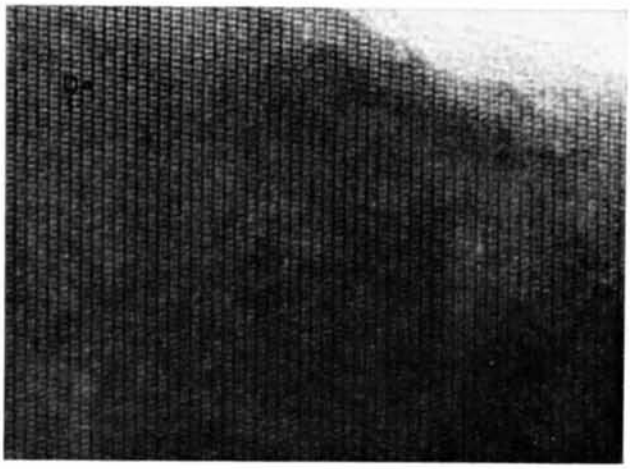

(*a*)

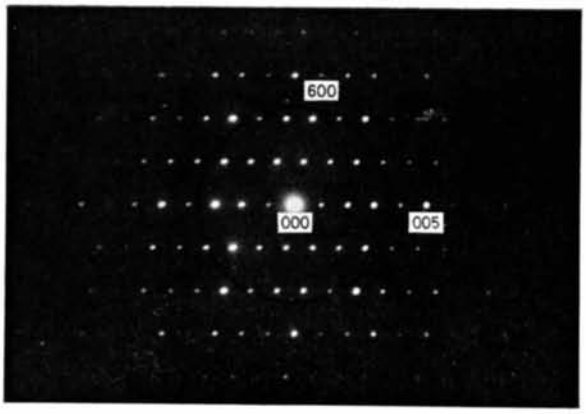

(*b*)

Fig. 2. (*a*) Lattice image of V_6O_{13}. The unit cell is outlined; $a=11{\cdot}9$ and $c=10{\cdot}2$ Å. (*b*) Electron diffraction pattern obtained from the area including Fig. 2(*a*). The circle represents the objective aperture used for taking the lattice image in Fig. 2(*a*).

[*To face p.* 660

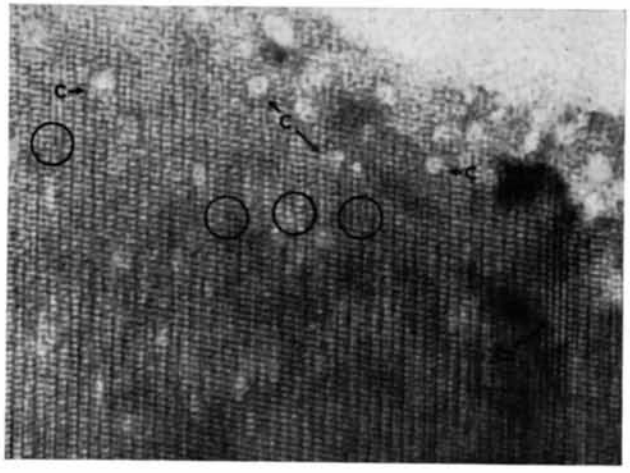

(*a*)

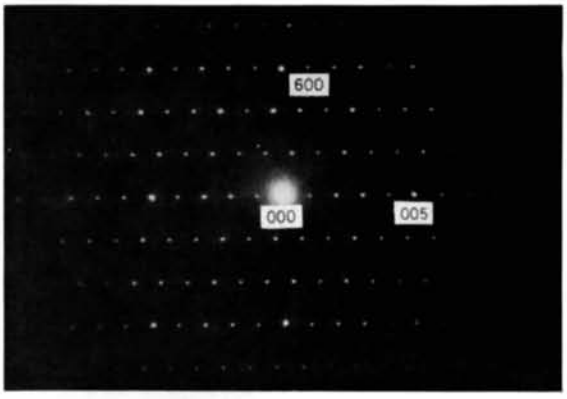

(*b*)

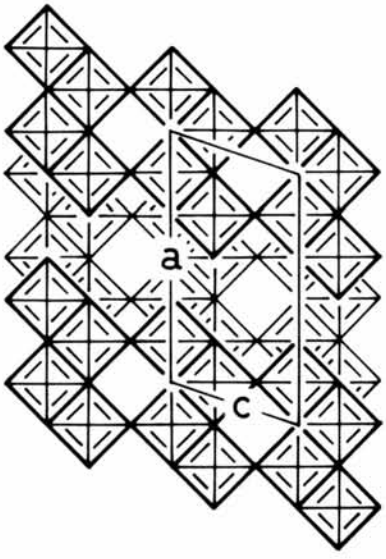

(*c*)

Fig. 3. (*a*) Initial stage of the intense irradiation of V_6O_{13}. White regions smaller than 20 Å in diameter appeared at the thin part of the crystal. Kinks in lattice fringes frequently occurred in the vicinity of the regions (parts *C*). They are clearly resolved in the encircled parts within the V_6O_{13} matrix. In the region *D*, a regular lattice image corresponding to a VO_2 phase appeared. (*b*) Corresponding diffraction pattern. (*c*) Structure model of the VO_2 phase.

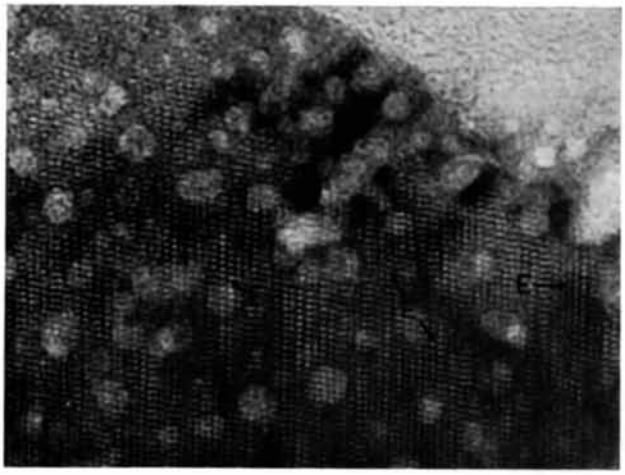

(*a*)

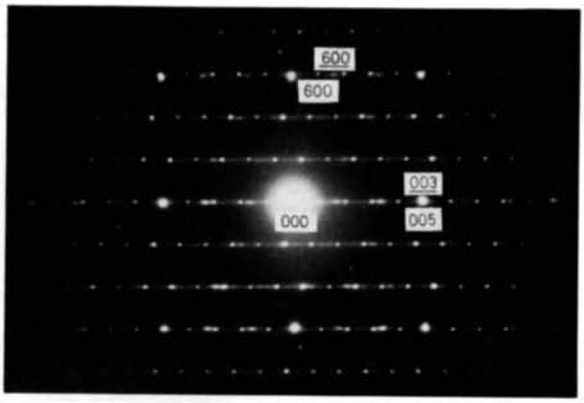

(*b*)

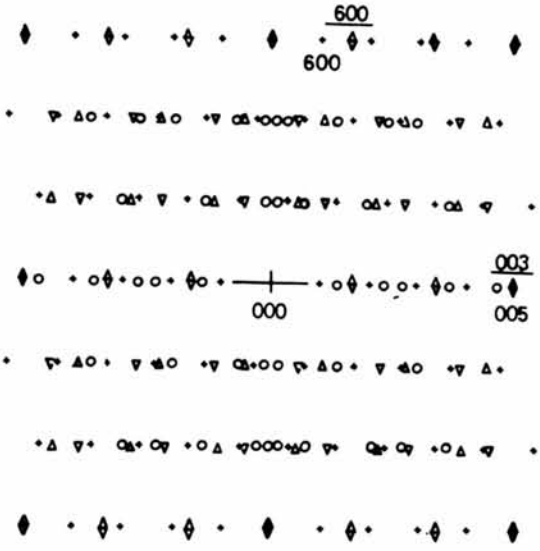

(*c*)

Fig. 4. (*a*) The advanced stage of reduction, induced by the electron-beam heating. The observed position is the same as in Figs. 2(*a*) and 3(*a*). The VO_2 phases are clearly resolved at parts *E*. (*b*) The diffraction pattern corresponding to Fig. 4(*a*). The reflexions $60\bar{1}$ (V_6O_{13}) and $\overline{60\bar{1}}$ (VO_2), or 005 (V_6O_{13}) and $\overline{003}$ (VO_2), overlap to give a strong intensity. That the diffraction spots of V_6O_{13} are sharp is considered to be due to the fact that they are obtained mainly from the part outside Fig. 4(*a*), where little reduction occurs. (*c*) Schematic representation of Fig. 4(*b*).

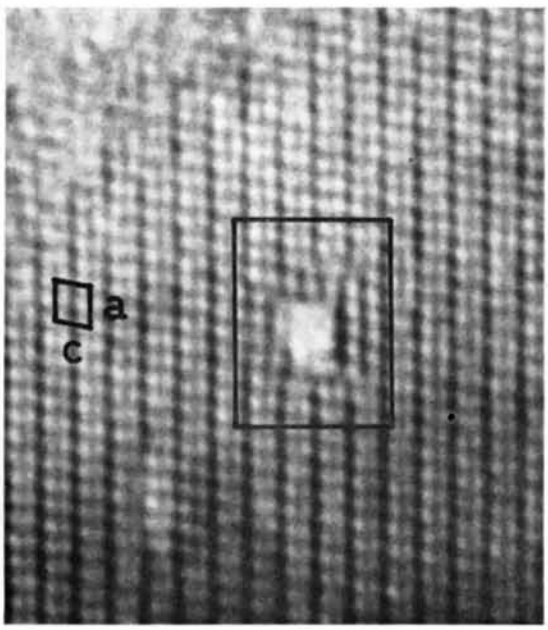

(*a*)

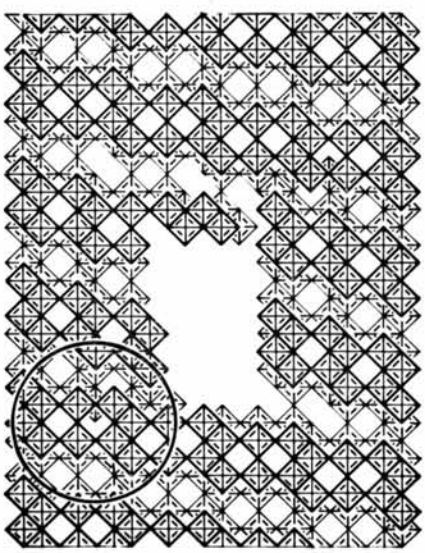

(*b*)

Fig. 5. (*a*) A structure observed at a very early stage of reduction, corresponding to a small white region in Fig. 3(*a*). (*b*) Schematic representation by VO_6 octahedra of the part outlined in Fig. 5(*a*).

beam in an electron microscope showed some structural changes. The changes were considered to be due to the reduction of the crystal, although the phases formed could not be identified as any of the above Magnéli phases.

Iijima, Kimura & Goto (1973) found that in the nonstoichiometric $Nb_{12}O_{29}$ crystal, whose oxygen partial pressure was measured to be about 1×10^{-12} Torr (Kimura, 1973), small black spots of about 5 Å in diameter disappeared during the observation with a high-intensity electron beam. They interpreted this as being due to the crystal reacting with the carbon deposited on the surface at an elevated temperature and being reduced to a stoichiometric composition.

In the present study the reduction of a V_6O_{13} crystal by the carbon deposit on beam heating is examined by means of high-resolution electron microscopy. According to the phase diagram (Kosuge, 1967) the V_6O_{13} phase has a narrow homogeneity range from room temperature to 708 °C, at which it melts. When it is reduced at a temperature lower than the melting point, the VO_2 phase of the rutile type should first be produced. Based on the thermodynamic data of Endo, Wakihara & Taniguchi (1974) the following can be stated: (1) The decomposition of V_6O_{13} into VO_2 and O_2 seems impossible, since it causes little change in the free energy of the system assumed present in an electron microscope. (2) The standard free energy for the reaction

$$2V_6O_{13}+C=12VO_2+CO_2 \qquad (1)$$

can be estimated to be about -73 kcal at 651 °C. It is therefore possible that the V_6O_{13} crystal reacts with the carbon deposit on heating by an electron beam. This is a reason for using the V_6O_{13} crystal in the present study.

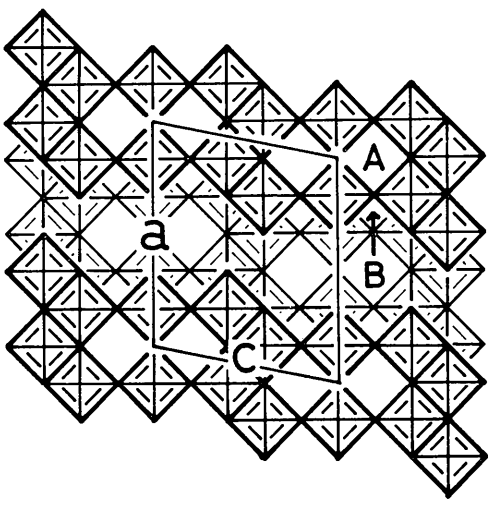

Fig. 1. Idealized structure of V_6O_{13} (Aebi, 1948). The darker and lighter squares represent the VO_6 octahedra, which form 2×3 blocks by their corner-sharing.

The phase contrast obtained by using a recent high-resolution electron microscope with a tilting apparatus approximately represents the potential distribution in the material observed (Cowley & Iijima, 1972). The array of metal ions in some complex oxides was really resolved and the method was successfully applied to identify such crystal imperfections as planar and point defects and to clarify the relationship with the nonstoichiometry (Iijima, 1971, 1973; Iijima, Kimura & Goto, 1973, 1974). Since the V_6O_{13} crystal has a block structure, as will be mentioned later, the array of VO_6 octahedra in the crystal and its change during the reduction are thought to be resolved in a lattice image by the high-resolution electron microscope. This is another reason for using the crystal.

Experimental procedure

Single crystals of V_6O_{13} were prepared by a chemical transport method (Saeki *et al.*, 1973). They are elongated plates of about 1 mm long and 0·2 mm wide. The lattice parameters were measured by X-ray diffraction to be $a=11{\cdot}9$, $b=3{\cdot}68$, $c=10{\cdot}2$ Å and $\beta=100{\cdot}9°$ (monoclinic).

The procedure to obtain high-resolution lattice images was the same as that reported by Iijima (1971). An HU 12A type electron microscope equipped with a goniometer stage ($\pm35°$ tilt) was used at an accelerating voltage of 100 kV with illumination from a pointed filament. The direct magnification was about 3×10^5. Exposure time was about 2 s. The specimen position was lowered by about 1 mm from the standard level in order to reduce the spherical aberration.

The lattice image was generally observed by using the aperture of the smallest size (300 μm in diameter) for the second condenser lens. The specimen was stable in the electron beam for a long time even at the maximum intensity. When another aperture of larger diameter was used and the electron beam was focused on the specimen, a structural change did occur. The rate of change depended on the intensity of the electron beam. The process could be observed in detail on the fluorescent screen through the optical magnifier ($\times10$). When the aperture was reset to the smallest size, the change immediately stopped. Photographs were then taken after recorrection of the astigmatism, the amount of defocus and the orientation of the crystal.

Results and interpretation

The crystal structure of V_6O_{13}, first determined by Aebi (1948) and later refined by Wilhelmi, Waltersson & Kihlborg (1971), is shown in Fig. 1; VO_6 octahedra form zigzag strings, extending along **b** by edge-sharing. The strings link together by corner-sharing, forming single sheets parallel to the *ab* plane. When two single sheets combine by edge-sharing, a double sheet, also parallel to the *ab* plane, is formed. These single and double sheets are joined by sharing addi-

tional corners and form a three-dimensional lattice of monoclinic symmetry.

Fig. 2(*a*) shows a lattice image of the V_6O_{13} crystal. A diffraction pattern obtained from this area coincides with the (010) reciprocal-lattice section, *i.e.* the electron beam is incident parallel to **b** [Fig. 2(*b*)]. Thick, dark lines, running along the *a* axis, correspond to the double sheets mentioned above (Horiuchi & Matsui, 1974). Dotted lines, running through the middle of them, correspond to the single sheets. White spots correspond to the tunnels running parallel to the *b* axis (marked *A* in Fig. 1). Although smaller tunnels (*B*) cannot be resolved, the array of VO_6 octahedra can be definitely assigned and the unit cell can be taken as that shown in Fig. 2(*a*). The angle between the *a* and *c* axes is about 101°, consistent with the structure model. Since there are no significant disturbances in the structure image, it can be said that the crystal is quite perfect. The specimen was stable in the electron beam as long as the smallest aperture was used for the condenser lens. The carbon deposited on the surface of the specimen owing to the breakdown of hydrocarbon vapours during the observation is seen as a film with a granular structure of about 20 Å in thickness.

The specimen was then irradiated by an electron beam of higher intensity with a larger bore for the condenser aperture. Some small white regions, in which no regular lattice image is observed, appeared at the beginning of the heating [Fig. 3(*a*)]. Most of them are smaller than 20 Å in diameter. They are preferentially formed at the thin part of the specimen. They are considered to be regions where the reduction of V_6O_{13} by the carbon begins. The lattice image of V_6O_{13} in the matrix region is not as regular as that shown in Fig. 2. Dark lines parallel to the *a* axis are still resolved, although they are often kinked. On kinking some planar defects in the **c*** direction must be formed. Fig. 3(*b*) shows a corresponding diffraction pattern. Each diffraction spot shows weak streaks parallel to **c*** due to such stacking faults.

In Fig. 3(*a*) another type of regular lattice image different from that of V_6O_{13} is also observed in the region *D*, extending along the *a* axis. From the image a structure model as shown in Fig. 3(*c*) can be deduced on the assumption that, by analogy with the image of V_6O_{13}, white spots represent the positions corresponding to the tunnels and dark lines the double sheets. The structure is constructed only of the double sheets, linked together by corner-sharing. The unit cell of this phase has monoclinic symmetry. The lattice parameters expected from the model are $a=11{\cdot}9$, $b=3{\cdot}68$, $c=6{\cdot}14$ Å and $\beta=107°$, while those measured from the image are $a=12$, $c=6{\cdot}4$ Å and $\beta=107°$. The atomic ratio V/O calculated from the model is $\frac{1}{2}$. The phase is thus established as being VO_2. However, in the diffraction pattern [Fig. 3(*b*)] no reflexion peaks from the VO_2 phase were observed. This is probably because the volume fraction was very low. The structural changes mentioned above were observed only in the thinner part of the specimen, while the thicker part still remained almost unchanged.

The specimen was heated further. The total time of heating by the intense electron beam amounted to about 2 min. Considerable changes in the image were observed not only at the thinner part but also at the thicker part of the specimen [Fig. 4(*a*)]. The image became very complicated locally and the VO_2 phase became predominant in volume. The lattice parameters measured from the image are $a=12$, $c=7{\cdot}1$ to $6{\cdot}2$ Å and $\beta=107°$.

Fig. 4(*b*) shows a diffraction pattern from the above specimen. The intensity of the streaks parallel to **c*** increased and some diffuse peaks appeared on the streaks. Fig. 4(*c*) is a schematic representation of Fig. 4(*b*). The distance between the diffuse peaks (upright triangles) is $\frac{5}{3}$ of that between the reflexions from V_6O_{13} (crosses). The peaks are reasonably explained on the basis of the model given in Fig. 3(*c*), since the lattice spacing of the VO_2 structure in the **c*** direction is $\frac{3}{5}$ of that of V_6O_{13}. On this basis diffraction spots were indexed in Fig. 4(*b*) and (*c*), in which the indices underlined refer to the VO_2 phase and those not underlined to the V_6O_{13} phase. That the *c* value of the VO_2 phase is not constant must be related to the fact that the intensity distribution of the diffuse peaks elongates along **c***.

In Fig. 4(*b*) some weak spots [inverted triangles in Fig. 4(*c*)] show the existence of the twin component of the VO_2 phase. The composition plane is parallel to the *ab* plane. The twin component was not resolved in the image probably because the image became complicated. Other diffuse peaks in Fig. 4(*b*) (circles) are interpreted as due to the double diffraction, *i.e.* some reflexions from the V_6O_{13} matrix excited near the centre spot are considered to act as new sources.

The specimen was tilted up to 55° about the *c** axis. It was observed on tilting that diffuse reflexion peaks always existed on the streaks parallel to **c***. The distance between these peaks with relatively strong intensity was always $\frac{5}{3}$ of that for V_6O_{13}. This observation confirms the structure of the VO_2 phase represented in Fig. 3(*c*).

The specimen was further irradiated after removal of the condenser aperture. It rapidly coagulated by melting. The temperature would certainly have exceeded 708°.

Discussion

The rate of structural change mentioned so far depended not only on the intensity of the electron beam but also on the duration used for setting the orientation of the crystal and for adjusting the astigmatism. If the duration was long enough to cause a thick carbon film to be deposited, the change proceeded at a fast rate when the beam was made more intense. On the other hand, a fresh crystal not covered by the carbon deposit does not show any change even under an

intense electron beam. These facts indicate that the carbon takes part in the reaction causing the structural change.

The crystal structure of VO_2 was reported to be of the rutile type (Westman, 1961). On the other hand, that found in the present study is of the monoclinic type and similar to that reported for $Na_{0.2}TiO_2$ (Andersson & Wadsley, 1962). In order to examine the effect of the carbon on the type of crystal structure the following experiment was undertaken; powders of V_6O_{13} and graphite were mixed in a molar ratio of 2:1, packed in the graphite crucibles and then heated in an evacuated furnace at temperatures from 500 to 650°C for 2h. The product was VO_2 of the rutile type with residual V_6O_{13} and graphite. The reason for the formation of the monoclinic VO_2 is unknown, since its thermodynamic data are not at hand. However, it is considered that they do not differ largely from those of the VO_2 of the rutile type and equation (1) (*see Introduction*) must still apply for the reduction in the electron microscope.

Stacking faults were frequently found in the vicinity of the white regions appearing at the initial stage of reduction [Fig. 3(*a*)]. Fig. 5(*a*) shows a very early stage of the change, where one small white region is enlarged. Fig. 5(*b*) is a schematic representation by octahedra of the part outlined in Fig. 5(*a*). Stacking faults are formed at both sides of the cavity created in the centre by the volume shrinkage and the array of octahedra is the same as that of VO_2. At the edge of the stacking faults kinks are formed and an example is encircled in Fig. 5(*b*). The cavity must extend along the *b* axis throughout the crystal and must be occupied by CO_2 gas and a small number of vanadium and oxygen atoms irregularly arranged. This view is also supported by the observation that the contrast is as weak as that of the tunnels in V_6O_{13}.

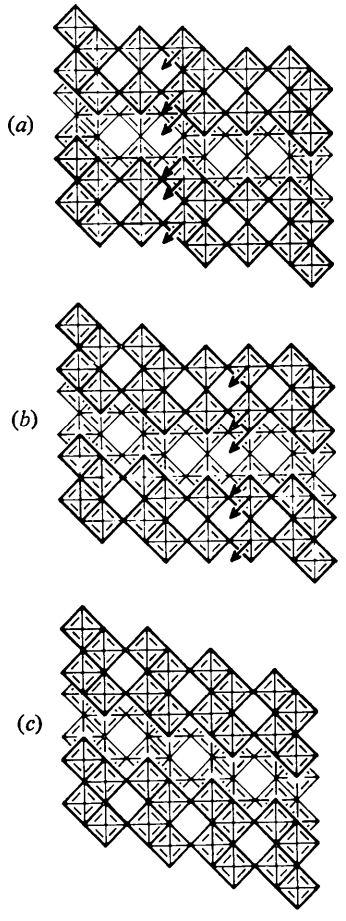

Fig. 6. (*a*)–(*c*). Schematic representation of the transition of V_6O_{13} to VO_2 by the cooperative movement of octahedra.

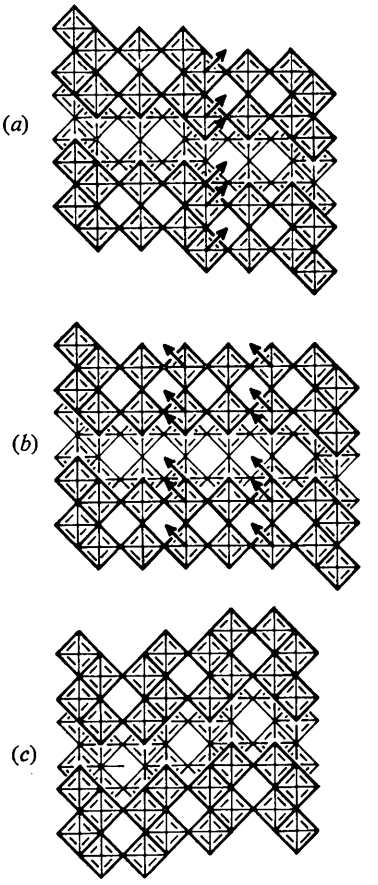

Fig. 7. (*a*)–(*c*) Schematic representation of the transition of V_6O_{13} to the twin component of VO_2.

The transition of V_6O_{13} to VO_2 is schematically shown in Fig. 6; half the number of octahedra in a double sheet first move cooperatively in the direction shown by the arrows [Fig. 6(*a*)] to form another double sheet at the adjoining plane [Fig. 6(*b*)]. This cooperative diffusion of octahedra (Andersson & Wadsley, 1966) causes only the movement of the shear plane and introduces little change in the enthalpy of the system. If further rearrangements of octahedra occur in the direction arrowed [Fig. 6(*b*)], a small

region of VO_2 phase composed of four adjoining double sheets is formed [Fig. 6(*c*)]. On the formation of VO_2 some oxygens are released and transferred by diffusion to the surface, where the reaction with the carbon deposit occurs. The free energy of the system is then lowered.

The formation process of the twin component of VO_2 is schematically shown in Fig. 7; a double sheet first decomposes into two single sheets [Fig. 7(*a*)]. If further movements of octahedra occur in the direction arrowed [Fig. 7(*b*)], a small region of VO_2 of a twin orientation forms [Fig. 7(*c*)]. As a result, some oxygens are released and the free energy of the system is lowered. The first stage of the process, *i.e.* the decomposition of a double sheet, seems, however, rather reluctant to occur because it must introduce a volume expansion of the matrix and because some oxygens must at once be absorbed. The transition to the twin component is therefore considered to be suppressed in comparison with that mentioned in relation to Fig. 6.

Browne, Hutchison & Anderson (1972) observed the oxidation process of $Nb_{12}O_{29}$ to Nb_2O_5 by means of electron diffraction and lattice images. Although no individual metal ions were resolved, the image contrast was interpreted to represent the array of 3×3 or 3×4 blocks produced during the phase transition. On the basis of the results obtained they proposed that any string of –Nb–O–Nb–O– atoms along the unique block axis moves in unison and that the oxidation reaction proceeds as a ripple of rearrangement of octahedra throughout the crystal. In the present study on the reduction it was found that the cooperative movement of octahedra also played an important role. However, it seems to be achieved not by the movement of atoms in unison but by the propagation of kinks appearing at the initial stage of the reduction process [Figs. 3(*a*) and 5(*a*)]; if the kinks located in the encircled part in Fig. 5(*b*) move downward along **a**, the rearrangement of octahedra as suggested in Fig. 6 can be achieved.

The authors wish to express their deep gratitude to Dr S. Yamaguchi (NIRIM) and Dr T. Komoda (Hitachi Central Research Laboratory) for their encouragement and to Dr M. Goto (NIRIM) for a valuable discussion.

References

AEBI, F. (1948). *Helv. Chim. Acta*, **31**, 8.
ANDERSSON, G. (1954). *Acta Chem. Scand.* **8**, 1599.
ANDERSSON, S. & WADSLEY, A. D. (1962). *Acta Cryst.* **15**, 201–206.
ANDERSSON, S. & WADSLEY, A. D. (1966). *Nature, Lond.* **211**, 581–583.
BROWNE, J. M., HUTCHISON, J. L. & ANDERSON, J. S. (1972). *Proceedings of the 7th International Symposium on the Reactivity of Solids*, Bristol, pp. 116–124.
COWLEY, J. M. & IIJIMA, S. (1972). *Z. Naturforsch.* **27a**, 445–451.
ENDO, H., WAKIHARA, M. & TANIGUCHI, M. (1974). *Chem. Lett.* No. 7, 905–908.
HORIUCHI, S. & MATSUI, Y. (1974). *Phil. Mag.* **30**, 777–787.
IIJIMA, S. (1971). *J. Appl. Phys.* **42**, 5891–5893.
IIJIMA, S. (1973). *Acta Cryst.* A**29**, 18–24.
IIJIMA, S., KIMURA, S. & GOTO, M. (1973). *Acta Cryst.* A**29**, 632–636.
IIJIMA, S., KIMURA, S. & GOTO, M. (1974). *Acta Cryst.* A**30**, 251–257.
KIMURA, S. (1973). *J. Solid State Chem.* **6**, 438–449.
KOSUGE, K. (1967). *J. Phys. Chem. Solids*, **28**, 1613–1621.
SAEKI, M., KIMIZUKA, N., ISHII, M., KAWADA, I., NAKANO, M., ICHINOSE, A. & NAKAHIRA, M. (1973). *J. Cryst. Growth*, **18**, 101–102.
STRINGER, J. (1965). *J. Less-Common Metals*, **8**, 1–14.
TILLEY, R. J. D. & HYDE, B. D. (1970). *J. Phys. Chem. Solids*, **31**, 1613–1619.
WESTMAN, S. (1961). *Acta Chem. Scand.* **15**, 217.
WILHELMI, K. -A., WALTERSSON, K. & KIELBORG, L. (1971). *Acta Chem. Scand.* **25**, 2675–2687.